DCT-based Channel Estimation for Single- and Multicarrier Communications[☆]

Fernando Cruz–Roldán[a,*], María Elena Domínguez–Jiménez[b], Gabriela Sansigre–Vidal[b], David Luengo[c], Marc Moonen[d]

[a]*Department of Signal Theory and Communications (EPS), Universidad de Alcalá, 28805 Alcalá de Henares (Madrid), SPAIN.*
[b]*Department of Matematics Applied to Industrial Engineering (ETSII), Universidad Politécnica de Madrid, 28006 Madrid, SPAIN.*
[c]*Department of Signal Theory and Communications (ETSIST), Universidad Politécnica de Madrid, 28031 Madrid, SPAIN.*
[d]*Department of Electrical Engineering (ESAT-STADIUS), KU Leuven, 3001 Leuven, BELGIUM.*

Abstract

We present a novel channel estimation technique based on discrete cosine transforms (DCT) useful to multicarrier and single carrier communications. This technique is particularly suitable for DCT-based transceivers, in which channel estimation is essential for designing a front-end prefilter at the receiver. The proposed channel estimation technique is based on the use of training symbols, symmetric in time-domain, known by both transmitter and receiver. We demonstrate that by imposing a whole-sample symmetry condition in the training symbol, the channel impulse response can be estimated in a straightforward way. The theoretical expressions to obtain the channel impulse response from the training symbol are also derived. Finally, this study is completed with several computer simulations to demonstrate the validity of the estimation technique.

Keywords: Multicarrier modulation, single carrier modulation, channel estimation, discrete cosine transform.

1. Introduction

Multicarrier and single-carrier modulation (MCM and SCM) with redundant data are the dominant medium-access techniques in modern broadband communications. Discrete Fourier transform (DFT)-based systems are most popular

[☆]This work was partially supported by the Spanish Ministry of Economy and Competitiveness through project TEC2012-38058-C03-01, and by the Spanish Ministry of Education, Culture and Sports through project PRX14/00147.

[*]Corresponding author
Email address: fernando.cruz@uah.es (Fernando Cruz–Roldán)

for MCM and SCM due to their simplicity and robustness against multipath or frequency selectivity fading. Channel estimation has a significant influence on the system performance, and hence it is essential for receiver design for 4G and future 5G networks [1, 2, 3, 4]. Several authors have studied channel estimation for DFT-based systems, and different approaches have been proposed in recent years, most of them collected in two interesting surveys [5, 6].

Based on the fact that DFT-based systems present some drawbacks, the use of alternative block transforms to perform MCM or SCM has been recommended. Among them, the discrete cosine transform (DCT) has been proposed to deal with the effects of carrier frequency offset (CFO) [7, 8, 9, 10]. The above works report the benefits of DCT-based energy compaction and the conditions to use this transform in MCM. One of these conditions is that the channel impulse response (CIR) has to be symmetric, and it is satisfied by including a front-end prefilter $\mathbf{h_{pf}}$ at the receiver. This is one of the main complexity disadvantages of DCT-based systems, since to design this front-end prefilter, the CIR must be known [7, 10]. As a result, the channel estimation is not only necessary to compensate for the channel effects, but also to construct this prefilter.

In this paper, a simple DCT-based CIR estimation technique is presented. We focus our attention on MCM, though the proposed solution also applies for SCM. Assuming that the time-domain channel $\mathbf{h_{ch}}$ can be modelled as an FIR filter, the proposed non-blind data aided channel estimation technique is based on the use of a whole-sample (WS) symmetric training symbol. We derive the formulation of the channel estimator for systems that employ a Type-IV even and Type-II even DCT (DCT4e and DCT2e), mainly motivated by their technological advantages (for more details refer to [7, 10]). However, this study can be easily extended to other classes of DCTs.

The rest of the paper is organized as follows. In Section 2, we describe the system model. In Section 3, we precisely formulate the problem, deriving expressions to estimate the CIR for DCT2e- and DCT4e-based systems. Section 4 presents some simulation results to demonstrate the validity of the proposed technique and to compare it with other DFT-based systems. Finally, Section 5 contains the conclusion.

2. MCM System Model

Figure 1 shows the general block diagram representing the transceiver and the channel estimation stage herein considered. At the transmitter, the incoming data $\mathbf{X}$ are processed by an N-point inverse transform $\mathbf{T}_a^{-1}$, with N being the number of subchannels or subcarriers. Then, matrix $\mathbf{\Gamma}$ introduces redundant samples into each time-domain data symbol

$$\mathbf{x}_e = \mathbf{\Gamma} \cdot \mathbf{T_a^{-1}} \cdot \mathbf{X}$$

in order to force the linear convolution performed by the channel to become a different convolution in the samples of interest ($0 \leq n \leq (N-1)$), equivalent to an element-by-element operation in the corresponding transform domain.

Ignoring for the moment the channel estimation stage, the received data vector can be specified as

$$\mathbf{y} = \mathbf{H} \cdot \mathbf{x}_e + \mathbf{z},$$

where $\mathbf{H}$ is a Toeplitz matrix formed from $\mathbf{h} = \mathbf{h_{ch}} * \mathbf{h_{pf}}$, and $\mathbf{z}$ is a column vector related to the additive noise. At the receiver, an $\boldsymbol{\Upsilon}$ matrix is needed to select the samples of interest and to allow the channel matrix diagonalization:

$$\mathbf{H}_{equiv} = \boldsymbol{\Upsilon} \cdot \mathbf{H} \cdot \boldsymbol{\Gamma} = \mathbf{T_c^{-1}} \cdot \mathbf{D} \cdot \mathbf{T_a},$$

where $\mathbf{D}$ is a diagonal matrix with elements d_i, $0 \leq i \leq (N-1)$. Next, a direct transform $\mathbf{T}_c$ is performed at the receiver

$$\mathbf{Y} = \mathbf{T}_c \cdot \boldsymbol{\Upsilon} \cdot \mathbf{y},$$

and the frequency domain equalization (FEQ) is carried out by means of one complex coefficient per subcarrier $1/d_i$.

In DMT and OFDM, $\mathbf{T}_a$ and $\mathbf{T}_c$ are DFTs. Furthermore, the insertion of redundancy, e.g., a cyclic prefix, allows the matrix $\mathbf{H}_{equiv}$ to be modelled as a right-circulant matrix, which can be expressed as

$$\mathbf{H}_{equiv} = \mathbf{W}^{-1} \cdot \mathbf{D} \cdot \mathbf{W}, \tag{1}$$

where $\mathbf{W}$ and $\mathbf{W}^{-1}$ are, respectively, the DFT and the IDFT matrix, and $\mathbf{D}$ is a diagonal matrix with elements d_i, obtained as the N-point DFT of the channel impulse response. On the other hand, when DCTs are employed as block transforms instead of DFTs, the insertion of redundancy such as a symmetric extension (SE) allows to convert $\mathbf{H}_{equiv}$ to the sum of a Toeplitz matrix and a Hankel matrix, which is diagonalized by the DCTs [7, 10].

3. DCT-based Channel Estimation

Let $\mathbf{h}_{ch} = [h_0, \cdots, h_\nu]^T$ be the transmission channel of length $\nu + 1$ and let

$$\mathbf{x}^{ps} = \left[\begin{array}{ccccccccccc} x_M & \cdots & x_1 & x_0 & x_1 & \cdots & x_M & 0 & \cdots & 0 \end{array} \right]$$

be the N-length training symbol to be transmitted. This symbol presents a WS symmetry in the nonzero samples, where $2M < N$ (see Fig. 2). Let us consider without loss of generality that $N = 2M + 2$. In this case, the $(N + 2M)-$length

received data vector is given by

$$\mathbf{y}' = \mathbf{X}_m \cdot \mathbf{h}_{zp} + \mathbf{z} = \begin{bmatrix} x_M & 0 & \cdots & 0 \\ \vdots & x_M & \ddots & \vdots \\ x_1 & \ddots & \ddots & 0 \\ x_0 & x_1 & \ddots & x_M \\ x_1 & x_0 & \ddots & \vdots \\ \vdots & x_1 & \ddots & x_1 \\ x_M & \ddots & \ddots & x_0 \\ 0 & x_M & \ddots & x_1 \\ \vdots & 0 & \ddots & \vdots \\ 0 & \ddots & 0 & x_M \end{bmatrix} \begin{bmatrix} h_0 \\ \vdots \\ h_\nu \\ 0 \\ \vdots \\ 0 \end{bmatrix} + \mathbf{z}, \tag{2}$$

where $\mathbf{X}_m$ is an $(N+2M) \times N$ matrix, and $\mathbf{h}_{zp}$ and $\mathbf{z}$ are $(N+2M) \times 1$ vectors, the latter one being related to the noise. The aim here is to express $\mathbf{h}_{zp}$ in terms of the received data vector $\mathbf{y}'$ and the training symbol $\mathbf{x}^{ps}$, known by the receiver. First, let us transform $\mathbf{X}_m$ into a square $N \times N$ equivalent matrix that can be diagonalized by a DCT4e or DCT2e, i.e., as the sum of a Toeplitz matrix and a Hankel matrix [11]. To this aim, the receving data must be multiplied as follows:

$$\mathbf{y}_r = \boldsymbol{\Upsilon}_{zp} \cdot \mathbf{y}',$$

where

$$\boldsymbol{\Upsilon}_{zp} = \begin{bmatrix} \mathbf{J}^M & \mathbf{I}^M & \mathbf{0} & \mathbf{0} & \mathbf{0} \\ \mathbf{0} & \mathbf{0} & \mathbf{I}^{(N-2M)} & \mathbf{0} & \mathbf{0} \\ \mathbf{0} & \mathbf{0} & \mathbf{0} & \mathbf{I}^M & \alpha \cdot \mathbf{J}^M \end{bmatrix}, \tag{3}$$

$\mathbf{I}^M$ denotes the $M \times M$ identity matrix, $\mathbf{J}^M$ is the $M \times M$ counter-identity matrix, and $\alpha = -1$ for DCT4e or $\alpha = 1$ for DCT2e. Then, the modified receiving data can be written as:

$$\begin{aligned} \mathbf{y}' &= \begin{bmatrix} \mathbf{J}^M & \mathbf{I}^M & \mathbf{0} & \mathbf{0} & \mathbf{0} \\ \mathbf{0} & \mathbf{0} & \mathbf{I}^{(N-2M)} & \mathbf{0} & \mathbf{0} \\ \mathbf{0} & \mathbf{0} & \mathbf{0} & \mathbf{I}^M & \alpha \cdot \mathbf{J}^M \end{bmatrix} \mathbf{X}_m \cdot \mathbf{h}_{zp} + \boldsymbol{\Upsilon}_{zp} \cdot \mathbf{z} \\ &= [\mathbf{X}_T + \mathbf{X}_H] \cdot \mathbf{h}_{zp} + \boldsymbol{\Upsilon}_{zp} \cdot \mathbf{z} = \mathbf{X}_{equiv} \cdot \mathbf{h}_{zp} + \mathbf{z}', \end{aligned} \tag{4}$$

where $\mathbf{X}_T$ is the Toeplitz matrix

$$\mathbf{X}_T = \begin{bmatrix} x_0 & \cdots & x_M & 0 & \cdots & 0 \\ \vdots & \ddots & \ddots & \ddots & \ddots & \\ x_M & & & & \ddots & 0 \\ 0 & & & & & x_M \\ \vdots & \ddots & \ddots & & & \vdots \\ 0 & \cdots & 0 & x_M & \cdots & x_0 \end{bmatrix}$$

and $\mathbf{X}_H$ is the Hankel matrix

$$\mathbf{X}_H = \begin{bmatrix} x_1 & \cdots & x_M & 0 & \cdots & 0 \\ \vdots & \iddots & \iddots & & \iddots & \vdots \\ x_M & \iddots & & & & 0 \\ 0 & & & & \iddots & \alpha \cdot x_M \\ \vdots & \iddots & & \iddots & \iddots & \vdots \\ 0 & \cdots & 0 & \alpha \cdot x_M & \cdots & \alpha \cdot x_1 \end{bmatrix}.$$

As a result, matrix $\mathbf{X}_{equiv} = \mathbf{X}_T + \mathbf{X}_H$ is square N-by-N and can be diagonalized by a DCT4e or by DCT2e, depending on the value of α.

For the DCT4e, $\alpha = -1$, we have:

$$\mathbf{C}_{4e} \cdot \mathbf{X}_{equiv} \cdot \mathbf{C}_{4e}^{-1} = \mathbf{D}_4.$$

Notice that $\mathbf{D}_4$ is a diagonal matrix [11], with the main diagonal defined as $\mathbf{d}_4^{ps} = \left[d_{4,0}^{ps}, \cdots, d_{4,N-1}^{ps}\right]^T$:

$$\mathbf{d}_4^{ps} = \mathbf{C}_{3e} \cdot \mathbf{x}_{ZP}^{ps,r},$$

where $\mathbf{C}_{3e}$ is the $N \times N$ type-III even DCT matrix, and $\mathbf{x}_{ZP}^{ps,r}$ is the $N \times 1$ vector defined as

$$\mathbf{x}_{ZP}^{ps,r} = [x_0, x_1, \cdots, x_M, 0, \cdots, 0]^T. \tag{5}$$

Using the result

$$\mathbf{y}_r = \mathbf{C}_{4e}^{-1} \cdot \mathbf{D}_4 \cdot \mathbf{C}_{4e} \cdot \mathbf{h}_{zp} + \mathbf{z}',$$

the CIR can be obtained in absence of noise ($\mathbf{z}' = 0$) as

$$\mathbf{h}_{zp} = \mathbf{C}_{4e}^{-1} \cdot \left((\mathbf{C}_{4e} \cdot \mathbf{y}_r) \,./ \mathbf{d}_4^{ps} \right),$$

where the operator ./ defines element-wise vector division:

$$[\mathbf{Y}./\mathbf{d}]_j = Y_j/d_j, \qquad 0 \le j \le (N-1).$$

On the other hand, for the DCT2e, $\alpha = 1$; $\mathbf{X}_{equiv}$ can be diagonalized by a DCT2e [11]:

$$\mathbf{C}_{2e} \cdot \mathbf{X}_{equiv} \cdot \mathbf{C}_{2e}^{-1} = \mathbf{D}_2.$$

Now, $\mathbf{D}_2$ is a diagonal matrix, with the main diagonal defined as $\mathbf{d}_2^{ps} = \left[d_{2,0}^{ps}, \cdots, d_{2,N-1}^{ps}\right]^T$, and obtained as the first N components of the $(N+1)\times 1$ vector defined as

$$\mathbf{d}_{2,N+1}^{ps} = \mathbf{C}_{1e} \cdot \mathbf{x}_{ZP}^{ps,r},$$

where $\mathbf{C}_{1e}$ is the $(N+1)\times(N+1)$ Type-I even DCT matrix, and $\mathbf{x}_{ZP}^{ps,r}$ is the $(N+1)\times 1$ vector defined as in (5). In this case, using the result

$$\mathbf{y}_r = \mathbf{C}_{2e}^{-1} \cdot \mathbf{D}_2 \cdot \mathbf{C}_{2e} \cdot \mathbf{h}_{zp} + \mathbf{z}',$$

the CIR can be obtained in absence of noise ($\mathbf{z}' = 0$) as

$$\mathbf{h}_{zp} = \mathbf{C}_{2e}^{-1} \cdot \left((\mathbf{C}_{2e} \cdot \mathbf{y}')\,./\mathbf{d}_2^{ps}\right).$$

4. Example Design

The capabilities of the proposed technique are examined in terms of symbol error rate (SER) and channel estimation error through computer simulations. The impact of the normalized CFO $\Delta f T$ on the SER is also considered. Fig. 1 shows the block diagram of the transceiver used in our experiments, in which we have considered the following configurations: a) OFDM system, in which $\mathbf{T} = \mathbf{T_a} = \mathbf{T_c}$ are DFTs; b) DCT4e-based system (DCT4e-MCM), in which $\mathbf{T_a} = \mathbf{T_c} = \mathbf{C_{4e}}$; c) DCT2e-based system (DCT2e-MCM), in which $\mathbf{T_a} = \mathbf{T_c} = \mathbf{C_{2e}}$. For the above, the corresponding matrices $\mathbf{\Gamma}$ and $\mathbf{\Upsilon}$ are defined in Table 1. Notice that in Fig. 1, $\mathbf{\Upsilon}_{zp} = \mathbf{\Upsilon}$ for the OFDM system, whereas (3) defines the matrix $\mathbf{\Upsilon}_{zp}$ for DCT-MCM.

The setup used in our experiments, summarized in Table 2, is similar to that in [10]. We have modelled frames that consist of 16 symbols. Regarding the OFDM system, the training symbols are inserted as in a block-type pilot channel estimation with all subcarriers used as pilots [13, 14]. A cyclic prefix (CP) is employed as redundancy, and the estimation is based on a least square (LS) criterion. As far as DCT-MCM is concerned, the training symbols are sent as the first symbol of each frame, using complex Zadoff-Chu sequences as defined in the LTE specifications [15], with length $2M + 1 = 511$. Zeros are appended as redundant samples to the training symbols (see Fig. 2). For the remaining 15 information symbols of each frame, SE is used as redundancy (see [10]). Finally, we consider that the channel does not change within a frame, but varies from frame to frame. Furthermore, we assume perfect synchronization and we have chosen the redundancy length to be greater than the channel order, which is assumed to be known, to avoid inter-symbol interference.

The front-end prefilter is not considered for OFDM, while it is implemented as the *time-reversed* (matched) filter to the estimated channel for DCT-MCM. According to this model, the estimated channel at the beginning of the frame is used to obtain the front-end prefilter and also to perform the equalization in the DCT domain.

Under the above conditions, the SER performances are shown in Figs. 3 and 4. It can be seen that a performance gap exists between DCT-MCM and

OFDM in the absence of carrier frequency offset (NCF) and under CFO, for the pedestrian A (pedA) and the vehicular A (vehA) channel. This performance gap is around 2.5 dB for SER values equal 10^{-3}. Moreover, the DCT2e-MCM system outperforms DCT4e-MCM and OFDM considering the veh A channel, high SNR, and CFO. Both DCT4e-MCM and OFDM exhibit a SER floor at high SNR for CFO=0.02.

We next compare the channel estimation performance using the mean squared error (MSE) and maximum error (MAXERROR), defined as in [16]. Figs. 5 and 6 show the obtained results for the veh A channel, with slight differences for NCF. In general, the estimation techniques improve for medium and high SNR and, on the contrary, DCT-MCM has a gain over OFDM under CFO.

5. Conclusion

Motivated by the lack of usable channel estimation methods for DCT-based systems, a novel channel estimator using DCT4e and DCT2e is presented. The major advantages of the proposed approach include better performance and that the same block transforms employed at both the transmitter and the receiver, can be used to carry out the channel estimation. The theoretical expressions to obtain the CIR estimate are derived when WS symmetric training symbols are transmitted. If the channel remains unchanged within one frame, there is no channel estimation error in the absence of noise. According to the performance comparison, the proposed method is a feasible channel estimation solution, since it achieves channel estimation performances better than the conventional OFDM systems.

[1] E. Kofidis, D. Katselis, A. Rontogiannis, and S. Theodoridis, "Preamble-based channel estimation in OFDM/OQAM systems: A review," *Signal Processing*, vol. 93, no. 7, pp. 2038 - 2054, July 2013.

[2] C. Qi, G. Yue. L. Wu, Y. Huang, and A. Nallanathan, "Pilot design schemes for sparse channel estimation in OFDM systems," *IEEE Transactions on Vehicular Technology*, vol. 64, no. 4, pp. 1493-1505, April 2015.

[3] H. Zhang and H.-C. Wu, "Robust pilot detection techniques for channel estimation and symbol detection in OFDM systems," *IEEE Signal Processing Letters* vol. 22, no. 6, pp.733-737, June 2015.

[4] H. Shu, E. P. Simon, and L. Ros, "On the use of tracking loops for low-complexity multi-path channel estimation in OFDM systems," *Signal Processing*, vol. 117, no. 12, pp. 174-185, Dec. 2015.

[5] Y. Liu, Z. Tan, H. Hu, L. J. Cimini, G. Y. Li, "Channel estimation for OFDM, " *IEEE Communications Surveys & Tutorials*, vol. 16, no. 4, pp. 1891-1908, Fourthquarter 2014.

[6] M. K. Ozdemir and H. Arslan, "Channel estimation for wireless OFDM systems," *IEEE Communications Surveys & Tutorials*, vol. 9, no. 2, pp. 18-48, Second Quarter 2007.

[7] N. Al-Dhahir, H. Minn, and S. Satish, "Optimum DCT-based multicarrier transceivers for frequency-selective channels," *IEEE Transactions on Communications*, vol. 54, no. 5, pp. 911-921, May 2006.

[8] P. Tan and N. C. Beaulieu, "A comparison of DCT-based OFDM and DFT-based OFDM in frequency offset and fading channels," *IEEE Transactions on Communications*, vol. 54, no. 11, pp. 2113-2125, Nov. 2006.

[9] F. Cruz-Roldán, M. E. Domínguez-Jiménez, G. Sansigre-Vidal, P. Amo-López, M. Blanco-Velasco, and Á. Bravo-Santos, "On the Use of Discrete Cosine Transforms for Multicarrier Communications," *IEEE Transactions on Signal Processing*, vol. 60, no. 11, pp. 6085-6090, Nov. 2012.

[10] F. Cruz-Roldán, M. E. Domínguez-Jiménez, G. Sansigre-Vidal, J. Piñeiro-Ave, and M. Blanco-Velasco, "Single-carrier and multicarrier transceivers based on discrete cosine transforms type-IV," *IEEE Transactions on Wireless Communications*, vol. 12, no. 12, pp. 6454-6463, Dec. 2013.

[11] V. Sánchez, P. García, A. M. Peinado, J. C. Segura, and A. J. Rubio "Diagonalizing properties of the Discrete Cosine Transforms, " *IEEE Transactions on Signal Processing*, vol. 43, no. 11, pp. 2631-2641, Nov. 1995.

[12] 3rd Generation Partnership Project, 3GPP TS 25.101, Technical Specification Group Radio Radio Access Network. User Equipment (UE) Radio Transmission and Reception (FDD) (Release 7), Sep. 2007.

[13] Y. Li, "Pilot-symbol-aided channel estimation for OFDM in wireless systems," *IEEE Transactions on Vehicular Technology,* vol. 49, no. 4, pp. 1207-1215, Jul. 2000.

[14] S. Coleri, M. Ergen, A. Puri, and A. Bahai, "Channel estimation techniques based on pilot arrangement in OFDM systems," *IEEE Transactions on Broadcasting,* vol. 48, no. 3, pp. 223-229, Sep 2002.

[15] 3rd Generation Partnership Project, 3GPP TS 36.211, Technical Specification Group Radio Radio Access Network. Evolved Universal Terrestrial Radio Access (E-UTRA), Physical Channels and Modulation (Release 10), 2010-2012.

[16] M. Blanco–Velasco, F. Cruz–Roldán, J. I. Godino–Llorente, J. Blanco–Velasco, C. Armiens–Aparicio, and F. López, "On the use of PRD and CR parameters for ECG compression," *Medical Engineering and Physics*, vol. 27, no. 9, pp. 798-802, Dec. 2005.

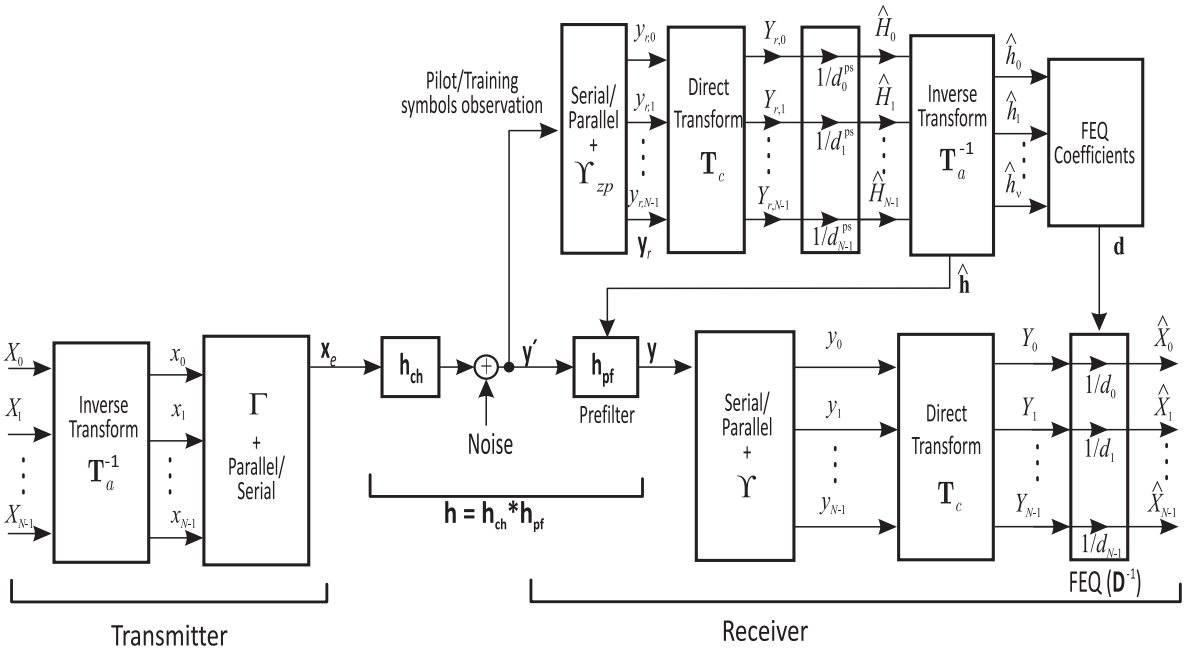


Figure 1: Block diagram of the transceiver systems used in the simulations.

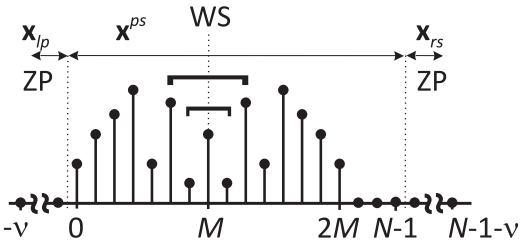


Figure 2: Symmetric training symbol with zero-padding. WS and ZP stand for, respectively, whole-sample symmetry and zero padding.

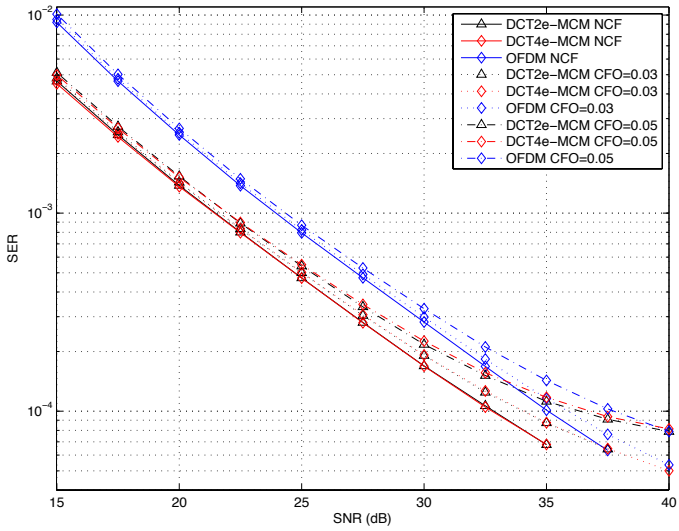


Figure 3: Symbol error rates with channel estimation for Ped A channel.

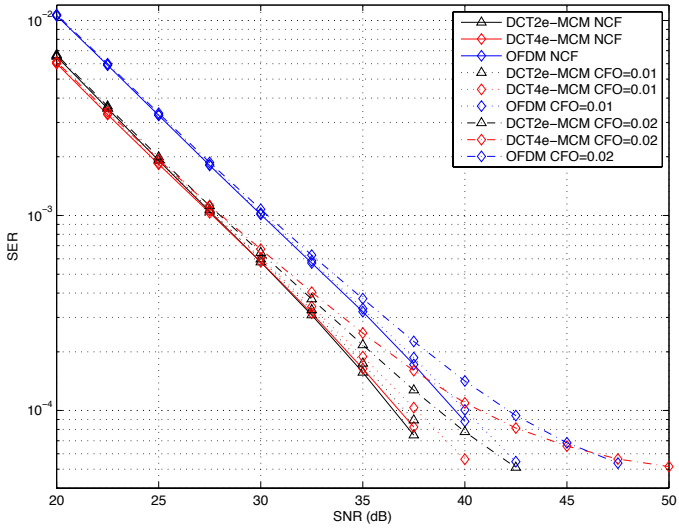


Figure 4: Symbol error rates with channel estimation for Veh A channel.

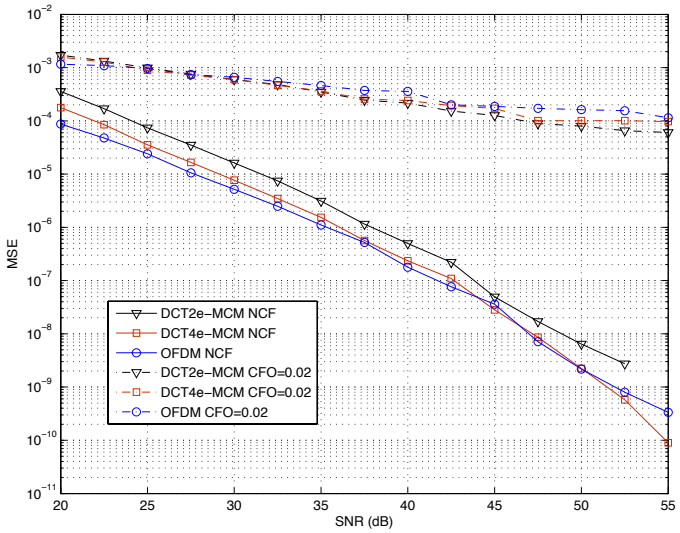


Figure 5: Channel estimation MSE versus SNR for Veh A channel.

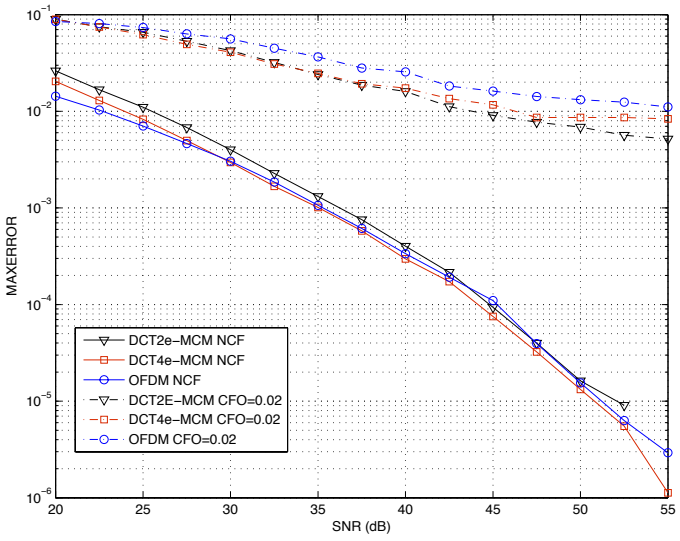


Figure 6: Channel estimation MAXERROR versus SNR for Veh A channel.

Table 1: Simulation Matrices ($\alpha = 1$ for DCT2e and $\alpha = -1$ for DCT4e).

	DFT	DCT
$\mathbf{\Gamma}$	$\begin{bmatrix} \mathbf{0}_{\nu\times(N-\nu)} & \mathbf{I}_{\nu\times\nu} \\ \multicolumn{2}{c}{\mathbf{I}_N} \end{bmatrix}$	$\begin{bmatrix} \mathbf{J}_{\nu\times\nu} & \mathbf{0}_{\nu\times(N-\nu)} \\ \multicolumn{2}{c}{\mathbf{I}_N} \\ \mathbf{0}_{\nu\times(N-\nu)} & \alpha\mathbf{J}_{\nu\times\nu} \end{bmatrix}$
$\mathbf{\Upsilon}$	$\begin{bmatrix} \mathbf{0}_{N\times\nu} & \mathbf{I}_N \end{bmatrix}$	$\begin{bmatrix} \mathbf{0}_{N\times\nu} & \mathbf{I}_N & \mathbf{0}_{N\times\nu} \end{bmatrix}$

Table 2: Simulation Parameters.

Parameters	Value
System Bandwidth	5 MHz
Sampling Period	200 ns
Carrier Frequency	2 GHz
Modulation and Demodulation	QPSK
Total Subcarrier Number (N)	512
Input Block Size	16 symbols
Length of Redundancy	32 (OFDM) 32×2, Left and Right Prefixes (DCT)
Channel Models	ITU Ped A (5 km/h) [12] ITU Veh A (120 km/h) [12]
Channel Equalization	Zero Forcing
Noise Model	iid AWGN
Detection	Hard Decision
Number of Transmitted Bits	$> 5 \cdot 10^6$
Number of Simulations	500